Project Report submitted to UGC Major Research project

Synthesis and Characterization of Transition Metal doped Spinel Compounds

Project code: F. No. 39-490/2010 (SR)(2011 – 2014)

Project Supervision ***Project Fellow***

Dr. Azher M. Siddiqui ***Alok Kumar Singh***

Project Report UGC Major Research project
(February 2011 - February 2014)

Synthesis and Characterization of Transition Metal doped Spinel Compounds

Principal Investigator : Dr. Azher Majid Siddiqui
Address : Faculty of Natural Sciences
Department of physics, JMI, De lhi-110025

Project code : F. No. 39-490/2010 (SR)
Date of joining of Project : 22, February 2011

Introduction

Spinel compounds are the group of minerals that are oxides of Magnesium, Iron, Manganese or Aluminium. The term spinel is derived from spina (Latin, thorn) in reference to its pointed octahedral, crystal habit. Spinel minerals are widely distributed in the earth, in meteorites' and in rock from moon.

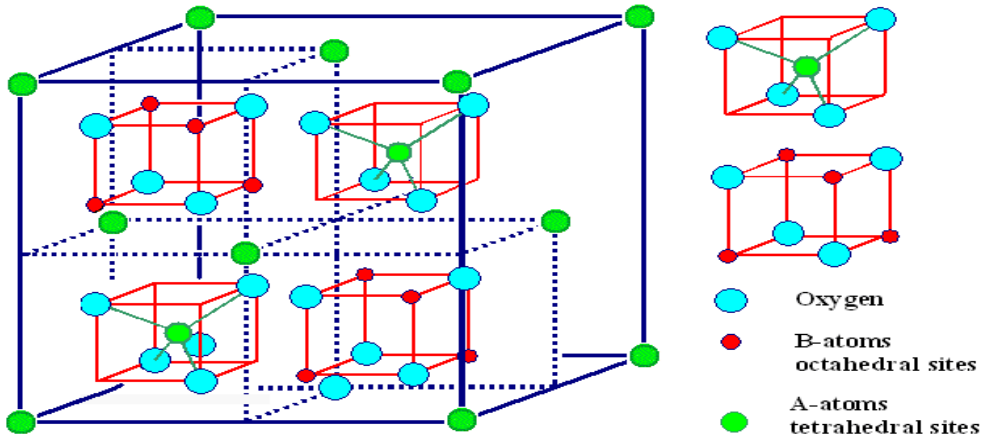

AB_2O_4 **spinel** The red cubes are also contained in the back half of the unit cell

Figure.1. Structure of Spinel compounds

While the ideal spinel formula is $MgAl_2O_4$, some 30 elements, with valence from 1 to 6, are known to substitute in the A and B cation sites, having the spinel crystal structure. The name spinel minerals that have so far been recorded in nature are oxides that occur as a matrix of A^{2+} versus B^{3+} cations.

The spinel series is evolved from the classification: Spinel, Magnetite and Chromite. These are very hard, variously colored minerals, having usually octahedral crystals and occurring in ignition and carbonates rocks. Spinels are very attractive subjects for material research and engineering applications.

Aluminous spinels are highly refractory, varying from translucent to transparent and from colorless to green, blue, brown and black. The compounds $MgAl_2O_4$ and Mg_2TiO_4 refers to the spinel structure type (space group F d 3m and Z=8). The magnesium aluminate spinel belongs to normal spinels, its formula is $(Mg^{2+})[Al_2{}^{3+}]O_4$.The round and square bracket denote the tetrahedral and octahedral sites respectively, while the oxygen ions are arranged in cubic closed packed structure.

Spinels also occur as a semiprecious gem and are widely employed as mechanically robust ceramic. The compass used in ancient time was a mixture of magnetite and meghemite. Enormous interest is paid to these spinel compound materials and the modification in their properties by various means for their uses in gems, radar, phase shifter, magnetic memory devices etc.

Literature Survey

Spinel compounds are attracting the researches from long time due to their interesting and useful properties. Spinel oxides AB_2O_4 as well as the perovskite oxides ABO_3 are ranked as one of the richest

groups in terms of the number of compounds and variety of physical properties. For instance, $LiTi_2O_4$, $MgTi_2O_4$, ZnV_2O_4 etc. Oxides display a variety of electromagnetic properties such as superconductivity [1], heavy fermion behavior [2–4], charge order [5], and unusual magnetic properties [6, 7].

N. Stubicar et al [8] have studied the dielectric and structural properties of MgO-TiO_2 and MgO-Al_2O_3 by powder mixing during high energy ball milling and post annealing. In their study they have observed that high energy dry ball milling is an efficient processing method even when used at the room temperature. It induces a structural change from the crystalline MgO-Al_2O_3 equimolar powder mixing to the compound $MgAl_2O_4$ crystalline single phases, if the mill processing was continued long enough. The formation process was complete after milling up to 10 h and no intermediary phase was detected.

The structural, synthesis and physical properties of spinel solid solution Mg_2TiO_4-$MgTi_2O_4$ has been studied by Masahiko Isobe et al [9]. They observed that transition metal oxide (spinel) possesses various properties such as superconductivity found in $LiTiO_2$, heavy fermion behavior in LiV_2O_4, charge ordering in AlV_2O_4 and unusual magnetic transition in ZnV_2O_4 and $ZnCr_2O_4$. Among transition metal spinel oxide, it is well known that $MgTi_2O_4$ is a candidate of spin (1/2) compounds with pyrochlore lattice, where novel quantum phenomena are expected.

Masahiko Isobe et al [10], have given a brief review of phase transition from metal to spin singlet insulator at around 260K, which is accompanied by the structural transformation from cubic to tetragonal. These oxides play a major role in the modifications of electromagnetic properties such as Superconductivity, Heavy fermions' behavior, Charge ordering and unusual magnetic property. Charge ordering is subject to strong frustration when differing valences are arranged on neighboring sites.

Heinrich Hohl et al [11], have studied the electrical and magnetic property of spinel solid solutions $Mg_{2-x}Ti_{1+x}O_4$, in range ($0 \leq x \leq 1$). They found that with increase in titanium content, the lattice of the cubic unit cell increases from a=844.00 (pm) to a maximum value of 850.66 (pm). Electrical properties evolve from insulating to low resistive semiconductor behavior. The magnetic properties of the solid solutions are mainly determined by a temperature dependent magnetic moment of Ti^{3+} in octahedral crystal field.

Experimental Plan

Spinel compounds $Mg_{2-X}\ Ti_{1-X}\ M_{2X}O_4$ (where M= Al, Ni etc) oxides have been synthesized by ball milling and post annealing at different temperatures to make the single phase spinel materials. The Sol-gel techniques will also be used for the sample preparation. Characterization of the materials will be done by various techniques such as XRD, SEM, resistivity and Magnetic susceptibility etc.

Summary of the work done so far

In the present investigation, Magnesium ortho titanate (Mg_2TiO_4), has been chosen as primary composition. It has been initially doped with transition metal oxide as well as other oxides. Firstly we have doped Mg_2TiO_4 with Aluminum oxide (Al_2O_3), to make the samples normal Spinel from Inverse Spinel. The composition we have to make is $Mg_{2-x}Ti_{1-x}M_{2x}O_4$, (where M = Transition metal compounds). Three different

compounds, Magnesium oxide (MgO), Titanium oxide (TiO_2) and Aluminum oxide (Al_2O_3), Nickel oxide (NiO_2) etc, have been chosen to explore their possible applications. The bulk compounds have been prepared by Solid State reaction technique and High Energy Ball milling technique with post- Annealing.

Solid State Reaction Technique

In this technique, the powder samples were prepared by a solid state reaction of mixture with an appropriate molar ratio of highly purity of MgO, Al_2O_3 and TiO_2. The stoichiometric amounts of the weighted mixture according to the required composition and grounded into fine powder in agate mortar. The resulting mortar powder was calcined at 1000 ºC for 12 h in air to remove moisture followed by furnace cooling down to room temperature. After this, the resulting materials heated were pressed to pelletize of 10 mm diameter and 2 mm thickness by applying a pressure of 10 KN/cm^2. In order to synthesize the compounds, the samples were placed into alumina boats and sintered upto 1450 ºC temperatures up to 24 h in air using conventional tube furnace followed by the cooling at room temperature.

High energy, Ball milling & post- Annealing

Samples have also been synthesized by ball-milling & post annealing technique. They were performed in air at room temperature in planetary micro-mill with Zirconium balls. The powders used were reagent grade MgO, Al_2O_3 and TiO_2 (anatase form). In one charge a mass of 2 g of the powder mixtures (with ratios: Mg: Ti = 1:1 and 2:1, and Mg: Al equals to 1:1) was prepared. Dry ball milling was carried out in containers (cylindrical in shape and having 45 cm^3 volume) with 14 balls (with 10mm in diameter). Six samples were prepared to follow the milling kinetics at time sequences of about 1 min, 10 min, 1 h, 3 h, 6 h and 10 h. Subsequent post-anneal processing of the milled MgO–TiO_2 samples was carried out in air employing a alumina boat and Muffle furnace. The annealing temperatures were selected within the temperature range 600 – 1200 °C.

Sol-gel Method

Reagent grade Magnesium nitrate ($Mg(NO_3)_2.6H_2O$), Nickel nitrate ($Ni(NO_3)_3.9H_2O$) and citric acid were used as starting materials. The nitrates were weighed according to the nominal composition of $MgNi_2O_4$, and then dissolved into ethanol solution in a beaker. After adding a designed amount of citric acid into 1:1 ratio, small amounts of ammonia solution were dripped to adjust the pH of the precursor solution. The precursor solution was dehydrated at 80 °C to form a sol, followed by a further heating at 150 °C to yield a gel. The resulting gel was pulverized and calcined at 650-750 °C for 2 h. The resultant powders were pressed into circular bars (30×4×4 mm^3) and disks (13 mm diameter and 2 mm thickness), respectively, and then sintered at 900 °C for 12 h in air.

Result & Discussion, Qandilite (Mg_2TiO_4)

A comparative study of the samples has been performed by various characterization techniques, such as surface electron microscopy (SEM) and X-ray diffraction (XRD).

Surface electron microscopy (SEM)

The surface morphological investigations of the compounds Mg_2TiO_4 were explored by SEM, revealing the presence of cubic structure of various sizes 1-2μm depending upon the annealing duration. It is well known crystallographic planes that form the surface, determine the shape of compounds and their crystal habits depend on the relative order of surface energy. This leads to the imperfect spherical surface in the final morphology.

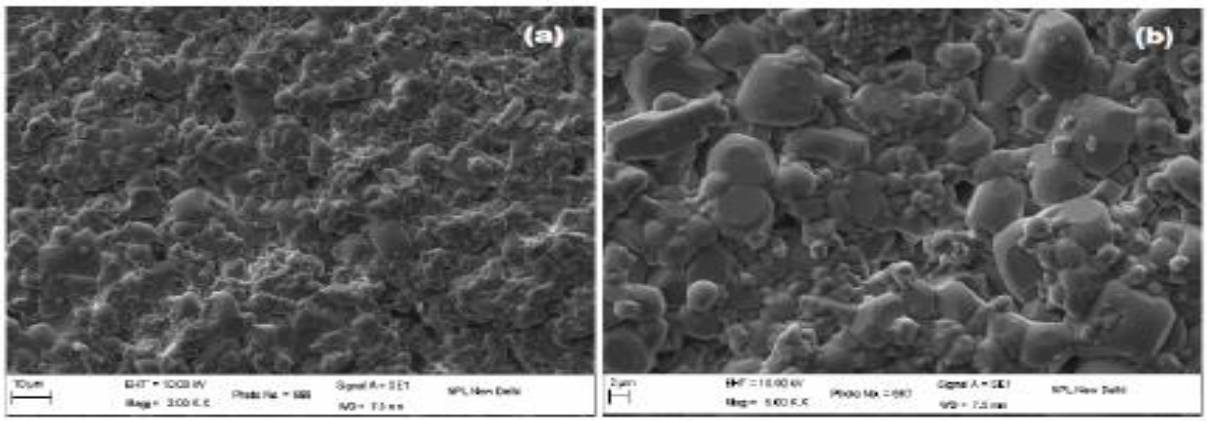

Figure.2. SEM images of the sample Mg_2TiO_4 with size (a) 10 μm and (b) 2 μm

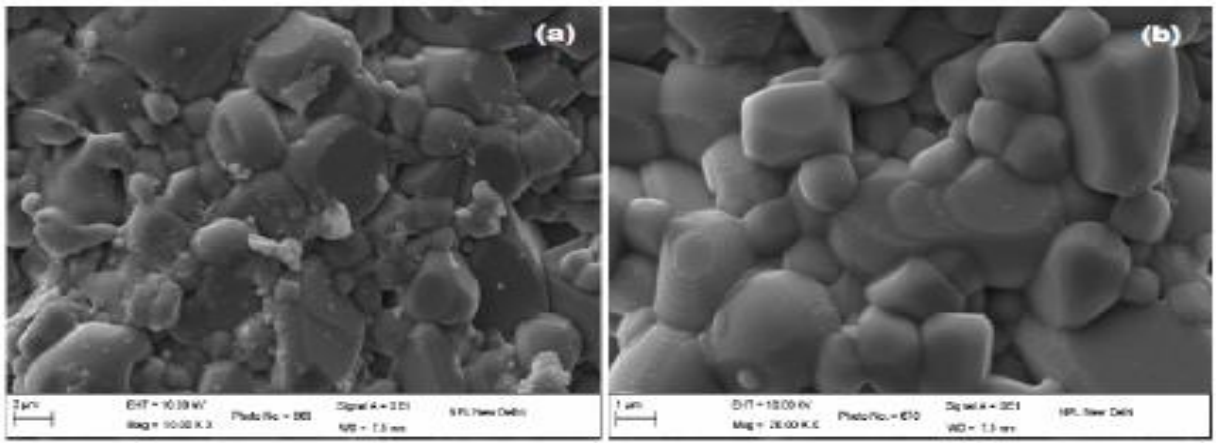

Figure.3. SEM images of the sample Mg_2TiO_4 with size (a) 2 μm and (b) 1 μm

Curious growth characteristics resembling a spiral like structures result in the large grain of Mg_2TiO_4. Fig. 3 (a & b) in the SEM micrograph reveals such features on Mg_2TiO_4 samples which was sintered at 1300 °C for 72 hours.

It also clearly demonstrates that how the nucleation of a new step takes place on an atomically smooth surface. These closed spiral growth loops in various shapes have been observed to be embedded invariably in all the large grain of synthesized Mg_2TiO_4.

Magnesium Ortho Titanate (Mg_2TiO_4) prepared by conventional solid state reaction technique, exhibits curious microstructural characteristics in the form of a myriad spiral like growth features.

These can be classified as:

1. Single cubic and circular spiral features

2. Interacting and interlaced circular and cubic spiral features

3. Spiral containing inclusion/platelet like features

4. Square spiral features truncated at the corners

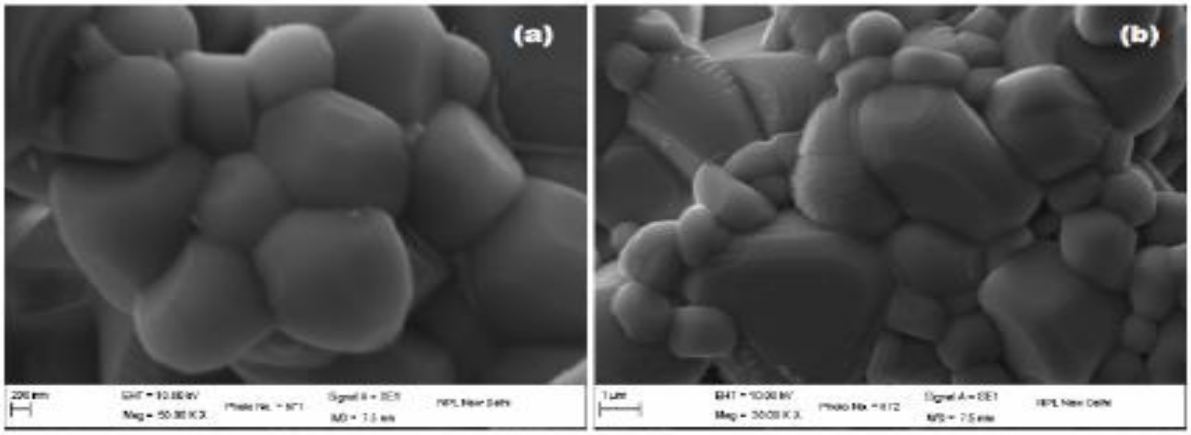

Figure.4. SEM images of the sample Mg_2TiO_4 with size (a) 200 nm and (b) 1 μm

A careful analysis of these samples which are sintered at 1300 °C for 72 hours shows cubical spiral features which are mediated through screw dislocation (figure above).

- **Study of curious spiral like features in inverse spinel compound (Mg_2TiO_4)**
  Alok Kumar Singh, *T. D. Senguttuvan and Azher M. Siddiqui*
  Int. J. Adv. Res. Sci. Technol. Volume 2, Issue2, 2013, pp 63-66.

X-Ray Diffraction Pattern

In order to investigate the effect of mechanical activation on the sample evolution, Mg $(NO_3)_2.6H_2O$ and TiO_2 powders were grounded for 10 Hrs, 15 Hrs, 24 Hrs and 48 Hrs sintered at 1300 °C for 72 hours. The evolved microstructure has been presented in fig. 5.

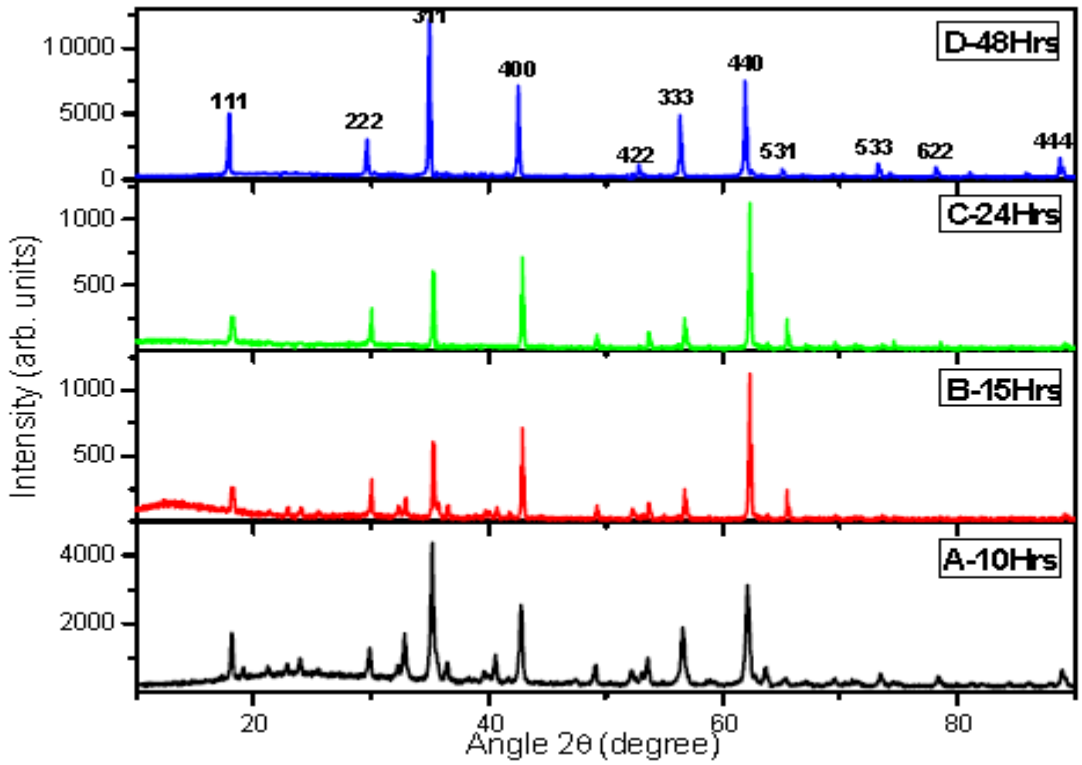

Figure.5. X- ray diffraction analysis of Mg_2TiO_4

Instead of using the present synthesis salts, one can use different salts of hydroxides, sulphates and oxide etc. as starting materials. However, the necessary condition to prepare pure single-phase material (Mg_2TiO_4) is to keep the ratio of Mg and Ti as 2:1. A careful analysis of XRD patterns of samples A, B, C and D reveals that structural changes were induced by ball milling and single phase formation takes place in sample D. The desired peaks are at 111, 222, 311, 400, 333 and 440.

This can be confirmed by the fact that for samples A, B and C, some extra peaks are observed indicating a mixed phase of $MgTiO_3$ and MgO. The XRD pattern was indexed using powder-X software which shows that the sample D-48 Hrs exhibits a cubic spinel structure with space group Fd3m and lattice parameter 8.42 Å.

Surface electron microscopy (SEM)

The morphological images of Mg_2TiO_4 samples grinded for (a) 10 Hrs (b) 15 Hrs (c) 24 Hrs and (d) 48 Hrs are shown in fig. 6.

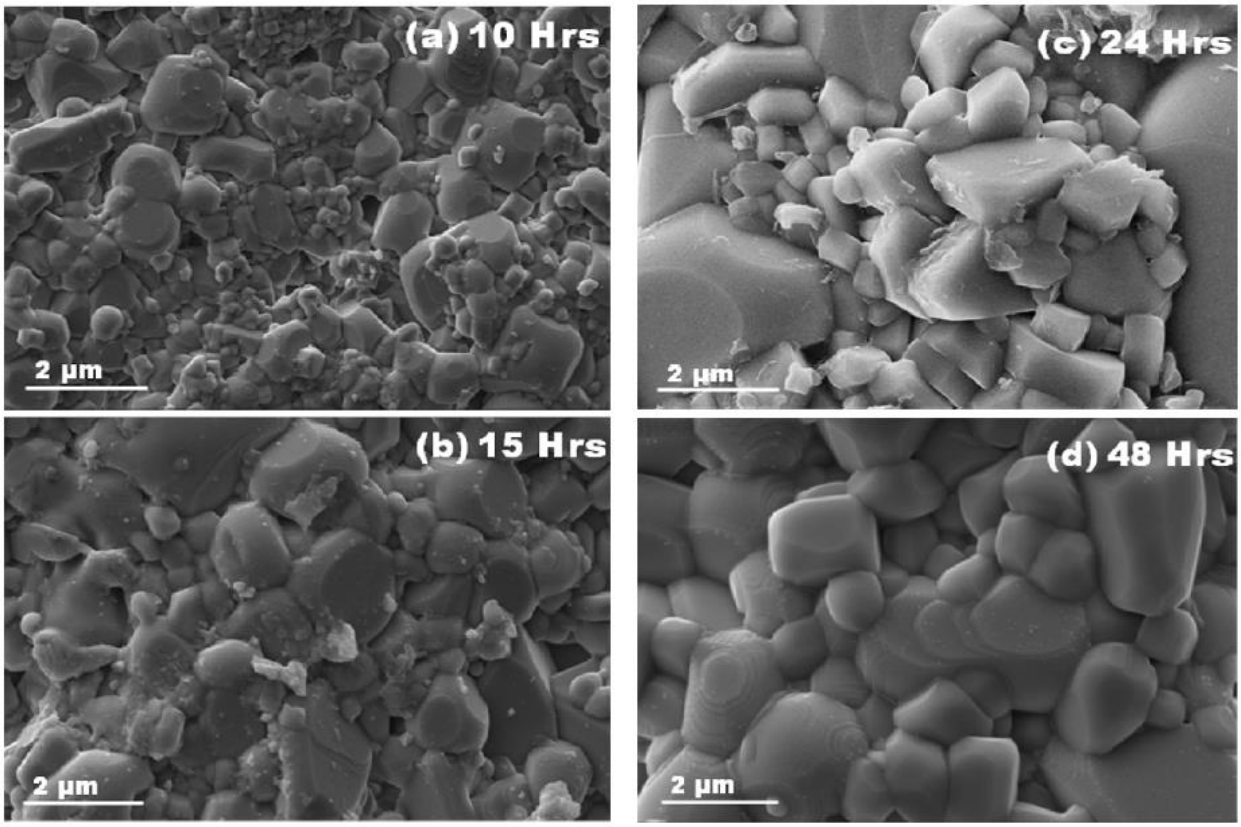

Figure.6. SEM images of pattern evolution in Mg2TiO4 samples grinded for (a) 10 Hrs (b) 15 Hrs (c) 24 Hrs and (d) 48 Hrs.

It has been observed in the micrographs that scattered and irregular structures of the material are becoming organized and well defined shape of three-dimensional structure as we proceed to the higher grinding time from 10 hrs to 48 hrs. The SEM results give the supporting evidence to the XRD results and shows that the increase in grinding time increases the refinement in the construction of the sample.

- **Synthesis, Microstructural and Thermal analysis of inverse spinel compound Mg_2TiO_4, *Alok Kumar Singh,* *T. D. Senguttuvan and Azher M. Siddiqui,Int. J. Adv. Res. Sci. Technol. Volume 2, Issue2, 2013, pp 95-97.***

Thermo Gravimetric Analysis and Differential Scanning Calorimetry:

The thermal behaviour of sample D has been studied by Thermo Gravimetric analysis & Differential Scanning Calorimetry (fig. 7). TG analysis reveals that the compound decomposes into two basic steps to produce the final binary oxide on heating in air. Fig. 7 also shows weight percentage and mass loss of the sample versus temperature.

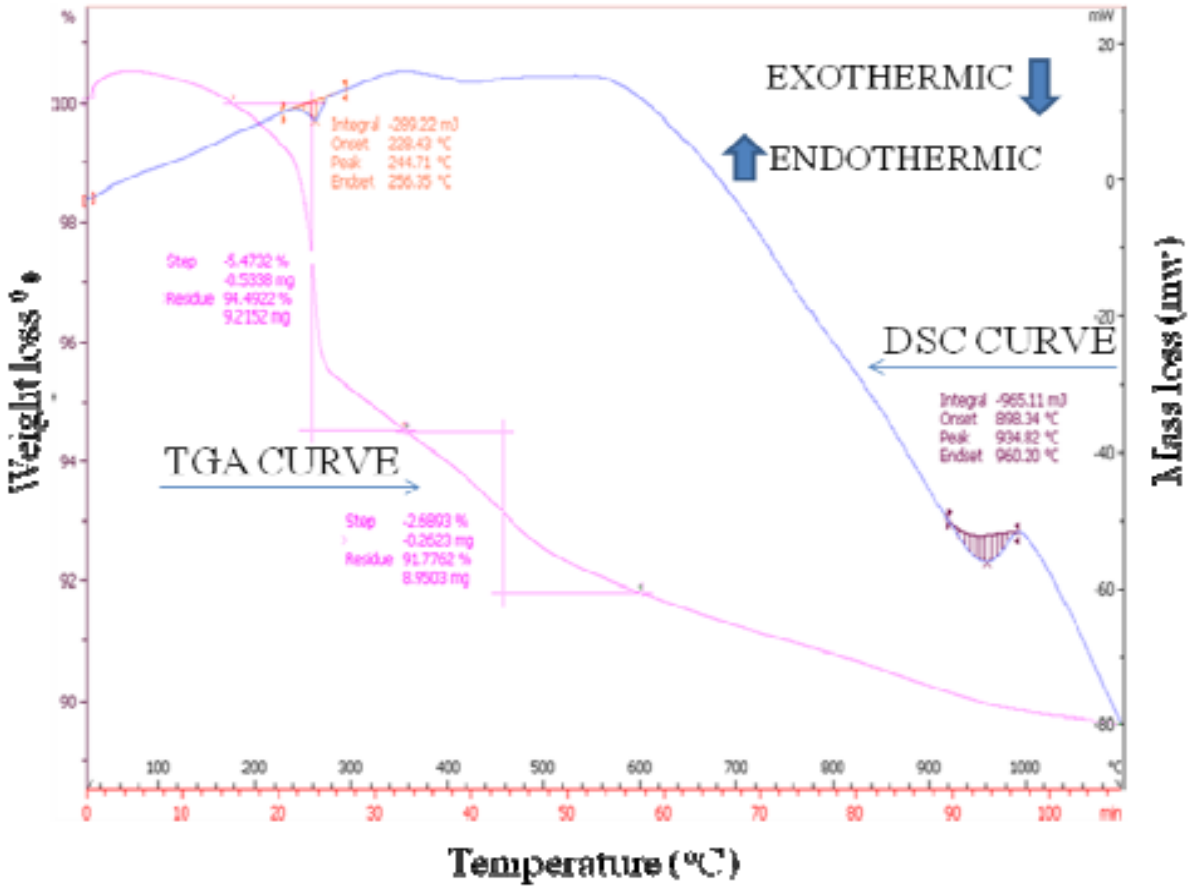

Figure.7. Thermo Gravimetric Analysis and Differential Scanning Calorimetry of Mg_2TiO_4

Two exothermic peaks appear at 244.71 °C and 934.82 °C. A residue of about 94.4922 % remains due to the elimination and suggestive of an abrupt mass loss assigned to the combustion of compounds. In the temperature range of about 450-550 °C we find the Magnesium ortho titanate (Mg_2TiO_4) phase. The material stabilizes at 600 °C and complete conversion of the molecular compounds takes place and a single phase binary oxide Mg_2TiO_4 forms.

Electrical Analysis

In order to determine the mechanism of conduction in spinels, usually the temperature dependence of the electrical conductivity is studied over the wide range of temperature. The conductivity can be assumed to consist of two parts, namely σB and σH, such that the total DC conductivity σdc = σB + σH. σB can be reported by the mechanism in the band conduction model for the high temperature, whereas σH is a

contribution due to charge transport at lower temperatures. The total conductivity of the ceramic was determined as the summation of the contributions from the two different conduction mechanisms.

The conductivity is expressed by

$$\sigma\,(T) \;=\; \sigma_1 \exp(-\,\Delta E/k_B T) \;+\; \sigma_o \exp[-(T_o/T)^{-1/4}] \qquad (1)$$

It is evaluated that at below 300 K, the charge transfer mechanism between localized states can be explained using Variable Range Hopping (VRH) model. The hopping conduction is associated with electron jumping from an occupied site to empty ones. The empty sites can be fulfilled at low temperatures. Hopping conductivity is governed by the hopping probability between occupied and unoccupied sites. At high temperatures, the hopping probability is dominated by the random spatial distribution of the atomic sites.

At higher temperatures, conductivity mechanism is mainly determined by hopping of carriers thermally activated into the band tails, as mono-energetic trap state becomes thermodynamically accessible at higher temperatures. In fact, the variable hopping regime dominating at lower temperature region should change to the constant range regime with increasing temperature because the hopping distance will reach its minimum possible value when the carriers jump between the nearest neighbor sites.

The ceramic indicates the typical behavior of a semiconductor as its electrical conductivity increases with increasing temperature. Similar behavior has been observed for the Mg_2TiO_4 and the variation of dc conductivity as a function of 1000/T in the temperature range 77-300 K is shown in Fig. 8.

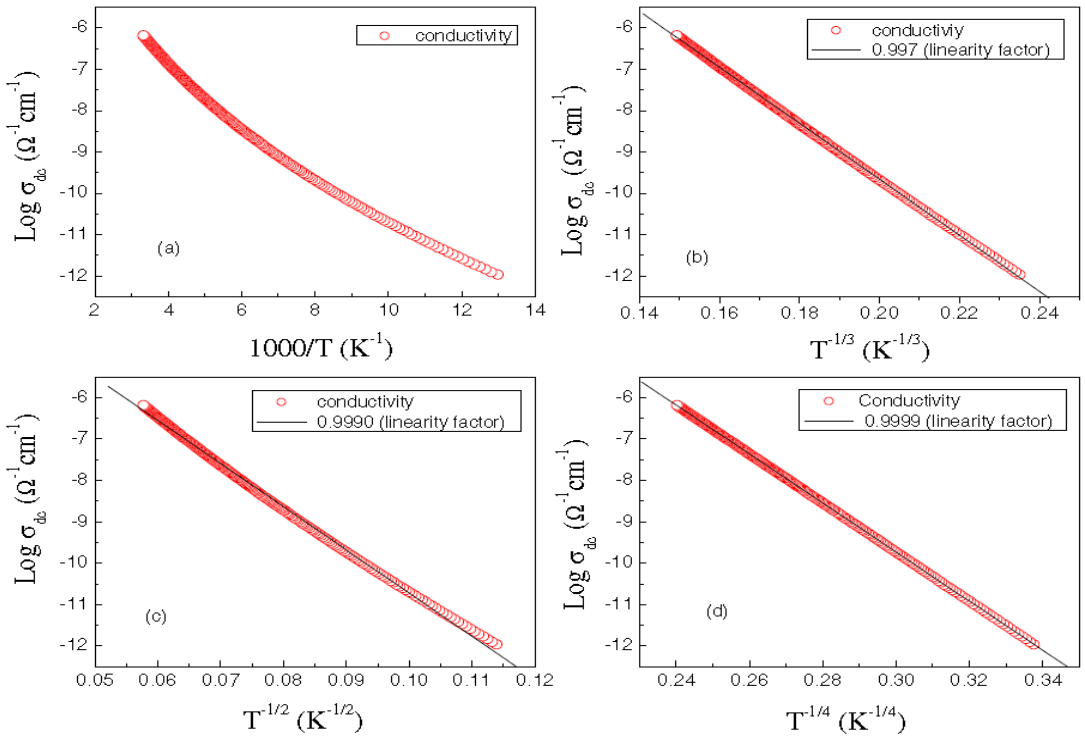

Figure.8. Variation in dc conductivity as a function of (a) 1000/T, (b) $T^{-1/2}$, (c) $T^{-1/3}$ and (d) $T^{-1/4}$ in the temperature range of 77– 300 K for Mg_2TiO_4

For the lower temperatures, the conductivity results have been examined in the light of Mott's variable range hopping (VRH) model. In this model, the dc conductivity shows the temperature dependence of type T^{-n} where n = 1/1+d, and d is the dimensionality. Therefore, Mott's model suggests n=1/2 for one

dimensional hopping, n = 1/3 for two dimensional hopping and n =1/4 for three dimensional hopping. From Figs. 8 (b), (c) & (d) the linear regression on the data points in entire temperature range of measurement gives the maximum linearity factor and hence best fit for $T^{-1/4}$ for the sample. So, 3D VRH seems to be a dominant charge transport mechanism.

- **Synthesis, Characterization and DC Conduction Mechanism in Inverse Spinel Compound (Mg_2TiO_4),** **Alok Kumar Singh,** Anju Dhillon, T.D.Senguttuvan and Azher M. Siddiqui, *Int. J. of Curr. Engg. and Technol.*, Vol.4, No.1 PP. 399-404.

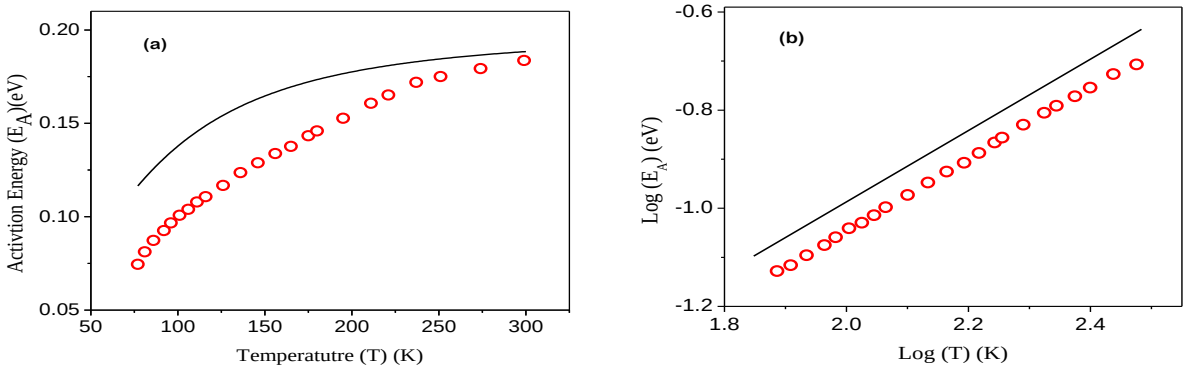

Figure.9. Plot of (a) activation energy E_A vs. temperature and (b) log activation energy vs. log temperature of Mg_2TiO_4.

Fig. 9(a) and 9(b) show the temperature dependence of activation energy, calculated from Fig. 8(a). The values of the activation energy along with that of dc conductivity at 300 K and 77 K are given in Table 1. The observed temperature dependence of activation energy

$$E_A = -\, d \ln\sigma / dT \qquad (2)$$

rules out band conduction at the low temperature.

Table 1. Dc conductivity (σ_{dc}) and activation energy (E_A) at 77 K & 300 K of Qandilite (Mg_2TiO_4)

Sample	Conductivity σ_{dc} ($\Omega^{-1}cm^{-1}$)		E_A (eV)	
	77K	300 K	77 K	300 K
Mg_2TiO_4	1.07×10^{-12}	6.52×10^{-7}	0.074	0.183

Mott has suggested that hopping may take place preferentially beyond nearest neighbors. The variable range hopping conductivity predicted by Mott and Davis, is of the form

$$\sigma_H = \sigma_o \exp\,[-(T_0/T)^n] \qquad (3)$$

where T_0 and σ_0 are constants and can be expressed as.

$$T_o = \lambda\alpha^3/k_B N(E_F) \qquad (4)$$

and

$$\sigma_o = e^2R^2\vartheta_o N(E_F) \qquad (5)$$

where T_o is the characteristic temperature, λ is a dimensionless constant and is assumed to be either 18 or 21, α is the coefficient of exponential decay of the localized states involved in hopping process. A reasonable

estimates for α is $\alpha=1/r_P$ where r_P is equivalent to the bond length in this system, i.e, 2 Å, as determined from the refinements of neutron and synchrotron diffraction patterns. K_B is the Boltzmann's constant, N (E_F) is the density of states at the Fermi level, e is the electronic charge, σ_0 is the conductivity at infinite temperatures, υ_0 is the phonon frequency (~1013Hz) and can be obtained from Debye's temperature θ_D, and R is the hopping distance between the two situations.

The plot in the temperature region where Eq. (3) is valid should give activation energy as per Eq. (2) and can be correlated to the parameters of Eq. (3) by the following equation

$$E_A=nk_BT_o(T_o/T)^{n-1} \quad (6)$$

It is evident from Eq.(6) that a plot of $\log E_A$ versus log T should yield a straight line of slope (n-1). The solid line corresponding to n=1/4 is shown in Fig. 9(b). It can be ascertained that the slope of the solid line is nearly parallel to obtain log activation energy data versus log T. This further indicates that three dimensional variable range hopping is dominant in the present case.

The temperature dependent activation energy can also be qualitatively explained if polaronic hopping is considered. According to Holstein, for orders material having polaronic hopping conduction, multiphonon processes are involved. These are gradually replaced at lower temperatures by the processes in which the only contribution to the jump frequency of the polaron is due to single optical phonon absorption or emission. The variation of activation energy for such a procedure is given by

$$\frac{E_{A'}}{E_A}=\frac{\left[tanh\left(\frac{\hbar\omega_0}{4k_BT}\right)\right]}{\left(\frac{\hbar\omega_0}{4k_BT}\right)} \quad (7)$$

where E_A is the room temperature activation energy, $\omega_0 = 2\pi\upsilon_0$, $\hbar = h/2\pi$, $E_{A'}$ is the activation energy for different temperatures. As a representative result, theoretical plot for $E_{A'}$ from Eq. (7) has been shown as solid line in Fig. 9(a) for the sample. It can be seen that the Polaronic hopping conduction can give temperature-independent activation energy, where multiphonon process dominates. Nevertheless, the temperature dependent activation energy rules out the above possibility, confirming the existence of Polaronic conduction through VRH where single photon processes are involved in the sample.

Furthermore, for Mott's theory to be applicable for the evaluation of hopping parameters a good fit of conductivity vs temperature data is essential. The hopping conductivity is given for the spinel in Fig. 4. The other hopping parameters which are hopping distance (R) and the average hopping energy (W) can be defined by the following relations:

$$R= [9/8\pi\alpha k_BTN(E_F)]^{1/4} \quad (8)$$

and

$$W= [3/4\pi R^3N(E_F)] \quad (9)$$

Mott's parameters T_0, R, W and $N(E_F)$ are given in Table 2.

Table 2. Calculated Mott's Parameters: characteristic temperature (T_0), density of states at Fermi level ($N(E_F)$), hopping distance (R) and average hopping energy (W), of Qandilite (Mg_2TiO_4).

Sample	T_0 (K)	$N(E_F)$(cm^{-3} eV^{-1})	R (cm)	W (eV)	αR
Mg_2TiO_4	$1.24x10^7$	2.53×10^{21}	10.22×10^{-8}	0.0881	5.11

The estimated values are consistent with the Mott's requirement that $\alpha R >> 1$ and $W >> k_BT$ for hopping to distant sites. The value of $N(E_F)$ is reasonable ($2.53x10^{21}$ cm^{-3} eV^{-1}), much below the Avogadro Number in the given range. From the above observations and subsequent calculations, it can be inferred that at lower temperatures the 3D VRH is the basic transport mechanism, whereas at higher temperatures the hopping probability is dominated by the random spatial distribution of the atomic sites.

Result & Discussion, Al-doped Qandilite (Mg_2TiO_4)

Surface electron microscopy (SEM)

It has been observed that surface structure becomes cubic as we sintered the sample at 1450ºC for 24 h as shown in fig.8.

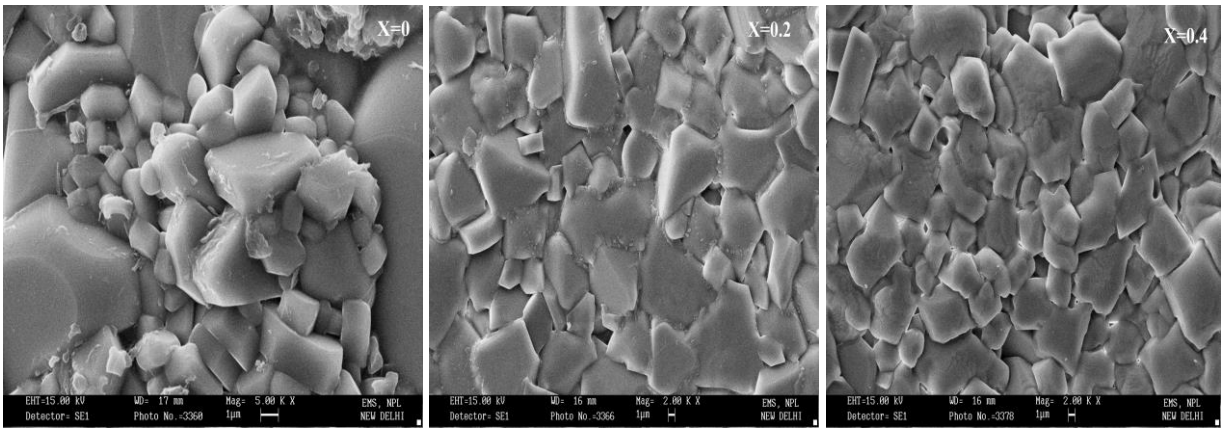

FIGURE.8. SEM image of $Mg_{2-x}Ti_{1-x}Al_{2x}O_4$, where (a) x = 0, (b) x = 0.2 and (c) x = 0.4

Figure.8 (a) indicates the cubical growth of product (x = 0, Mg_2TiO_4) and 2b ($Mg_{1.8}Ti_{0.8}Al_{0.4}O_4$) & 2c ($Mg_{1.6}Ti_{0.4}Al_{0.8}O_4$) indicates the tetragonal growth of $Mg_{2-x}Ti_{1-x}Al_{2x}O_4$. On sintering the sample for 24 hrs, the grains of size less than 1μm were achieved. It is clear from these images that the sample changes its phase from cubic to tetragonal as the dopant concentration is increased from x = 0 to x = 0.4. This is evident from the irregular growth pattern of the final product.

X-ray diffraction pattern

XRD patterns of the $Mg_{2-x}Ti_{1-x}Al_{2x}O_4$ are shown in Fig.9. It is observed that Mg_2TiO_4 have cubic structure (x = 0), where as phase transition from cubic to tetragonal is seen in Al-doped Mg_2TiO_4 (x = 0.4) (Fig.9). Reaction temperatures of at least 1300ºC were necessary to obtain single-phase material. The structure of the sample synthesized at 1450ºC was found to be cubic, with lattice parameter 842.00 pm for x = 0 and a = b 836.00 pm, c = 842.00 pm for x = 0.4 (tetragonal).

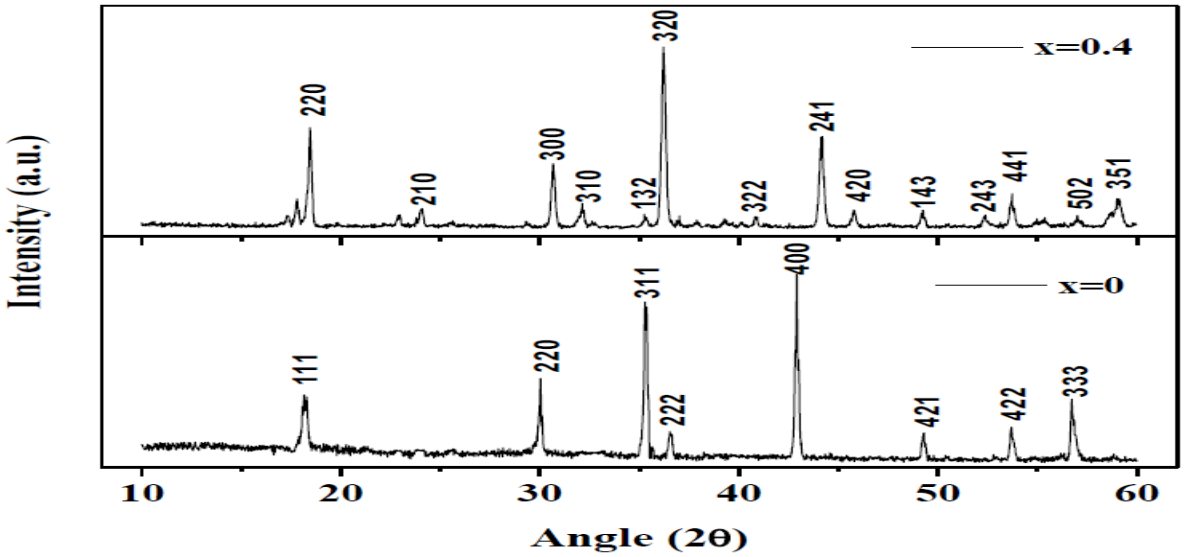

FIGURE.9. XRD pattern of $Mg_{2-x}Ti_{1-x}Al_{2x}O_4$, (where x=0 and 0.4)

Along with shifts in the peak positions, the transition from inverse to normal spinel structure with increasing aluminum content causes changes in relative peaks intensity, most apparent for the 220, 222, 311 and 400 peaks positions.

- **Synthesis and Structural Analysis of Al-doped Qandilite (Mg_2TiO_4)**
  Alok Kumar Singh, Ravi Kumar, T.D. Senguttuvan and Azher M. Siddiqui
  AIP Conf. Proc. 1393, pp. 235-236.

Result & Discussion, Ni-doped Qandilite (Mg_2TiO_4)

Nano-particles of $Mg_{2-x}Ti_{1-x}M_{2x}O_4$ ferrite were prepared by using citrate gel auto combustion method. The chemical reagents used in this work were Magnesium nitrate hexahydrated (Mg $(NO_3)_2 \cdot 6H_2O$) and Nickel nitrate hexahydrated (Ni $(NO_3)_2 6H_2O$) as starting materials. All the chemicals were of Merck. We use citric acid $C(OH)(COOH)(CH_2 \cdot COOH)_2 \cdot H_2O$ (M.W = 210.14) in this method because citric acid is a weak acid and has three carboxylic and one hydroxyl group for coordinating metal ions and therefore enhances the homogeneous mixing. Citric acid helps for the homogenous distribution and segregation of the metal ions. During water dehydration, it suppresses the precipitation of metal nitrates because it has electronegative oxygen atoms interacting with electropositive metal ions. Therefore, at a relative low temperature the precursors can form a homogenous single phase. The ammonia is used to adjust the pH for improving the complication, gel formation and also to improve the solubility of metal ions. Metal nitrates taken in the required stoichiometric ratio were dissolved in a minimum amount of ethyl alcohol and mixed together. The mixed metal nitrate solution was then added to the citric acid solution in 1:1 molar ratio. The pH value of the clear solution thus obtained was unity. Analytical grade liquor ammonia was then added drop-wise under constant stirring in order to reach the pH of the solution up to 6. The resulting solution was continuously heated on the magnetic stirrer at 40 °C in order to allow gel formation. The gel so formed is kept on hot plate at 80 °C for 7 h in order to remove the adsorbed water. During this process the gel swells into a

feathery mass, which eventually breaks into frail flakes. This precursor powder was then calcined at 600 °C for 12 h to obtain final product. The rate of heating and cooling was maintained 5°/min. The resultant powders were grind into fine particles using an agate mortar and pestle. The resultant powders were pressed into circular bars (30×4×4 mm^3) and disks (13 mm diameter and 2 mm thickness), respectively, and then sintered at 900 °C for 12 h in air. The structural characterization of all samples was carried out by Rigaku X-ray diffractometer (Rigaku Miniflex II) using the CuKα radiation (wavelength λ = 1.5406 Å). Scanning electron microscopy (SEM) images were obtained using a LEO 440 microscope. The composition was determined by energy dispersive X-ray spectroscopy (EDX, Inca Oxford, attached to the SEM). For the SEM and EDX measurements, the nano-particles of $Mg_{2-x}Ti_{1-x}M_{2x}O_4$ spinel were dispersed homogeneously in ethanol using ultrasonic treatment. A minute drop of nano-particles solution was cast on to a glass slide followed by subsequently drying in air before transfer it into the microscope.

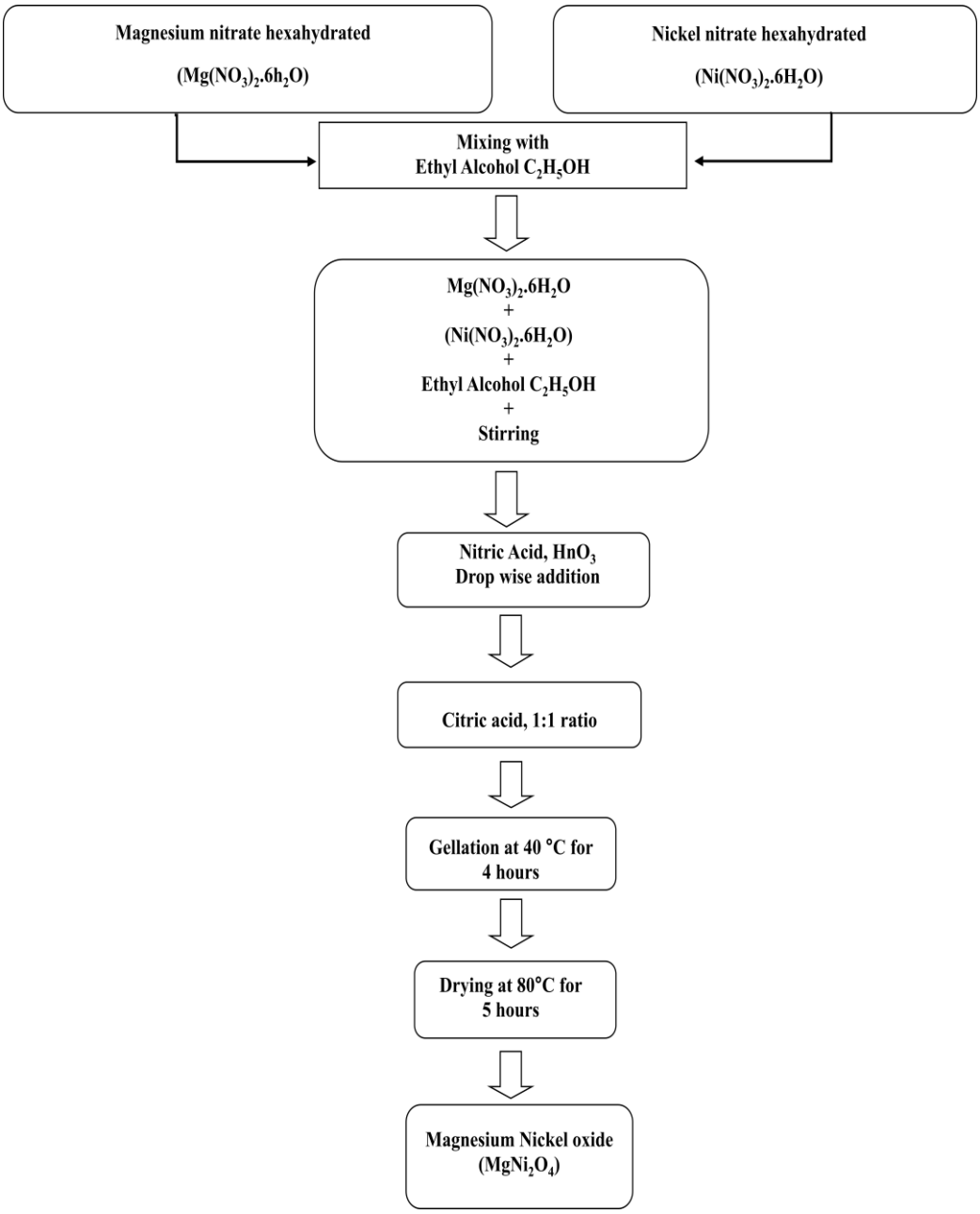

Fig. 10. Systematic diagram of the synthesis of magnesium nickel oxide ($MgNi_2O_4$)

Structural properties:

Fig. 11 highlights the XRD patterns of $Mg_{2-x}Ti_{1-x}M_{2x}O_4$ (where M = Ni), spinel nano-particles which exhibit single phase cubic spinel structure and exclude the presence of any undesirable secondary phase. Moreover, the broadening of the XRD peaks indicate that $Mg_{2-x}Ti_{1-x}M_{2x}O_4$ (where M = Ni), spinel have nano-crystalline behavior. The crystallite size of $Mg_{2-x}Ti_{1-x}M_{2x}O_4$ (where M = Ni) nano-particles were calculated from the most intense peak (330) of XRD data, using Debye Scherrer formalism:

$$t_{hkl} = \frac{0.98\,\lambda}{\beta_{hkl}\,Cos\theta_{hkl}}$$

Where $\beta = \beta_M^2 - \beta_i^2$. Here λ is X-ray wavelength (1.54 Å for Cu Kα), β_M and β_i are the measured and instrumental broadening in radians respectively and θ is the Bragg's angle in degrees.

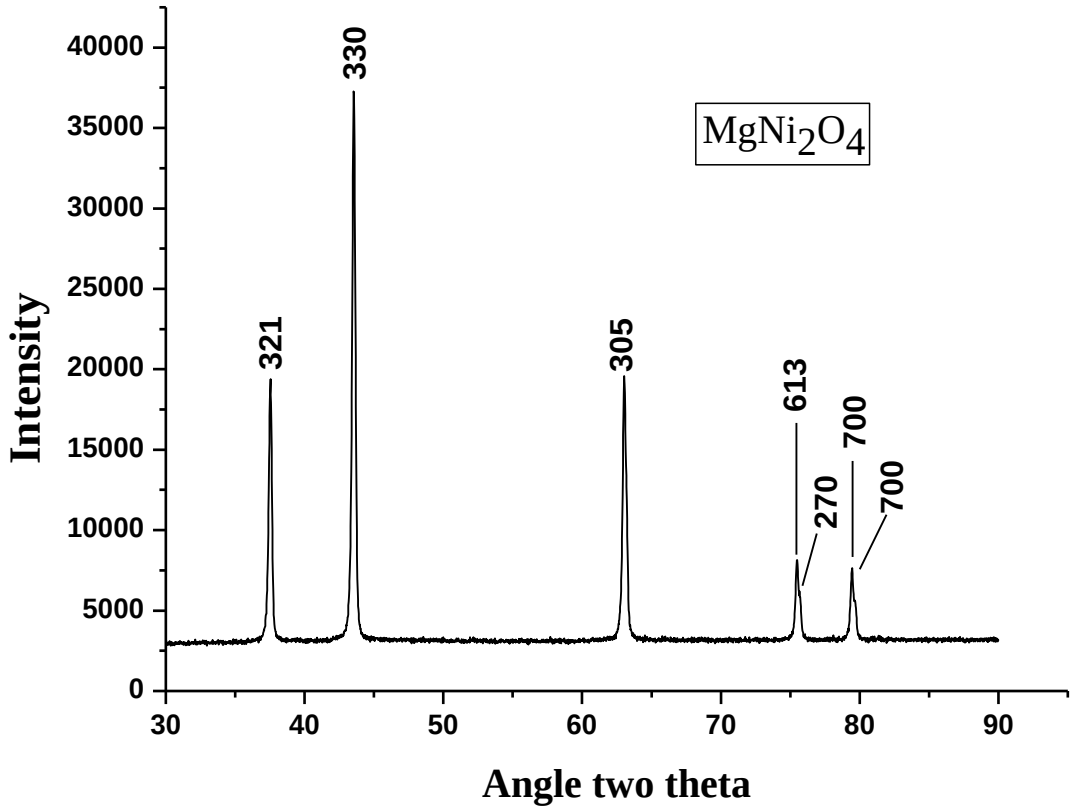

Fig.11.

X-ray Diffraction pattern of single phase ($Mg_{2-x}Ti_{1-x}M_{2x}O_4$, x = 1) $MgNi_2O_4$

The calculated value of particle size is shown in table 3, which implies that Ni doping favour the particle growth. The lattice parameters were calculated using Powder-X software was found to a = 8.4328 Å, b = 9.2345 Å, c = 8.6493 Å (see Table 3).

The X-ray density (theoretical) is calculated by using the following relation:

$$D_{hkl} = 8m/Na^3$$

Where M is the molecular weight of the compound, N the Avogadro's number, 'a' lattice constant and 8 represents the number of molecules per unit cell.

The apparent density (experimental) of the circular shape pellet is calculated by using the following relation:

$$D = \frac{m}{V} = \frac{m}{\pi h r^2}$$

where m, V, r and h represent the mass, volume, radius and the thickness of the pellet, respectively.

Table.3. Structural properties of $Mg_{2-x}Ti_{1-x}M_{2x}O_4$ spinel nano-particle

Composition	**Lattice Parameter (Å)**	**Crystalline size (nm)**	**Density (g/cm^3)**		**Porosity (%)**
			D(tho)	**D(exp)**	
$Mg_{2-x}Ti_{1-x}M_{2x}O_4$ (Where M = Ni)	a = 8.4328 Å, b = 9.2345 Å, c = 8.6493 Å	86.74 nm	4.056	3.184	21.50

The X-ray density depends on the lattice constant and the molecular weight of the sample, while the theoretical density of the samples is calculated from the geometry and mass of the samples. The X-ray density is higher than the apparent density. This may be due to the existence of pores in the sample, which depends upon the sintering conditions. Table 3 also shows the variation of the porosity of samples with composition. X-ray density decreases with Ni substitution, which may be due to the fact that the density and atomic weight of Ni are 8.912 g/cm3 and 58.6934, respectively. The apparent densities of the samples show the same general behavior like that of the theoretical density. The higher value of X-ray density than that of the apparent density is due to the existence of pores that depend on the sintering condition.

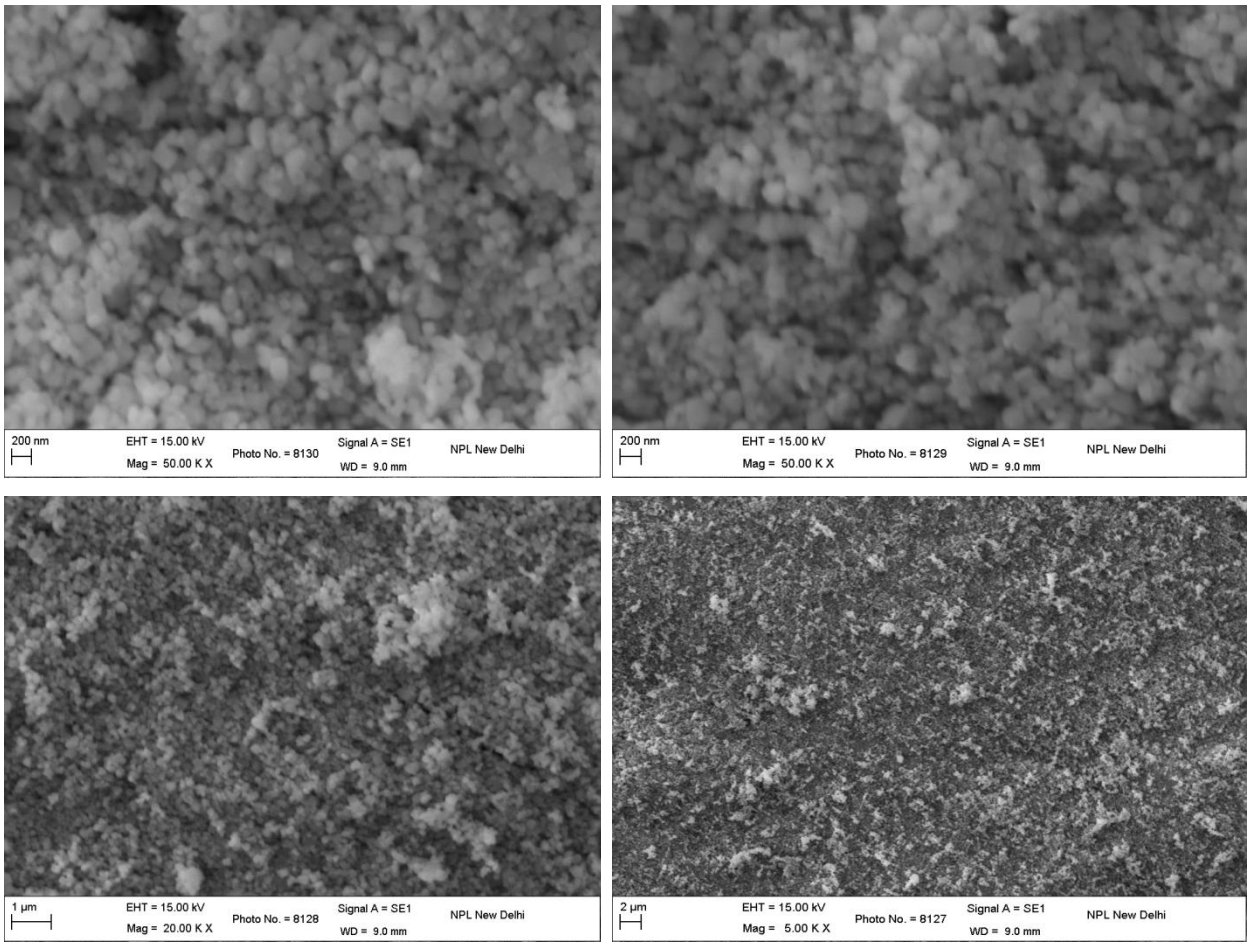

Fig.12. SEM micrograph of ($Mg_{2-x}Ti_{1-x}M_{2x}O_4$, where x = 1) $MgNi_2O_4$ at different scales

Fig. 12 shows the SEM micrographs of $Mg_{2-x}Ti_{1-x}M_{2x}O_4$ spinel nano-particles. It can be seen from the micrographs that all sample is composed of nano crystallite. Micrographs also show the uniform grain growth with Ni substitution and a decrease in porosity. It is clear from the micrographs that all the samples have the spherical shape crystallite with agglomeration and highly dense clusters are found with doping concentration.

The chemical compositions of $Mg_{2-x}Ti_{1-x}M_{2x}O_4$ spinel nano-particles have been calculated by EDX. Fig. 13 shows the EDX pattern for the various compositions of $Mg_{2-x}Ti_{1-x}M_{2x}O_4$ nano-particles. EDX measurements were carried out on the same point with electrons to give the chemical composition of essentially the core of the particle.

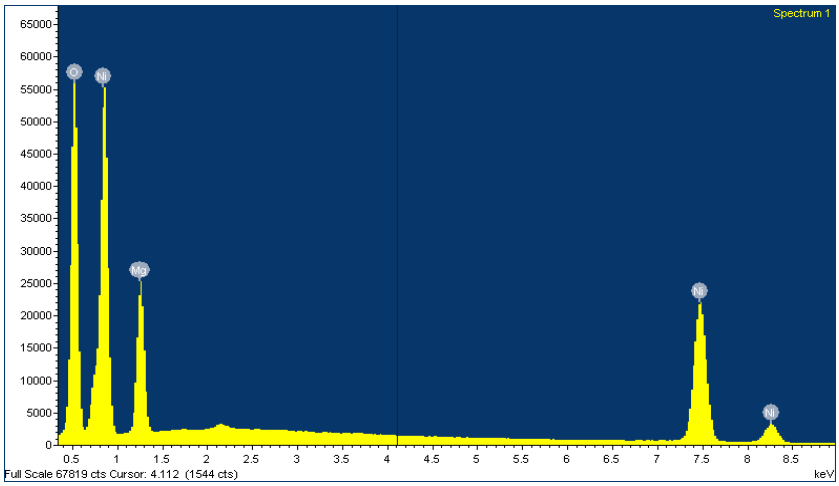

Element	Weight %	Atomic %
O K	25.42	50.96
Mg K	10.73	14.15
Ni K	63.85	34.88
Totals	100.0	

Fig.13. EDX pattern of ($Mg_{2-x}Ti_{1-x}M_{2x}O_4$, where x = 1) $MgNi_2O_4$ nano-particle

The peaks of the elements Mg, Ni, and O were observed and have been assigned. Since for EDX measurements the nano-particles of $Mg_{2-x}Ti_{1-x}M_{2x}O_4$ were dispersed on glass slide. The atomic weight percentages of various cations in the $Mg_{2-x}Ti_{1-x}M_{2x}O_4$ (x = 1.0) samples are found to be O^{2-} (50.96 %), Mg^{2+} (14.15 %) and Ni^{2+} (34.88 %) The calculated percentage of Ni value matches well with the amount of Ni used in the respective precursors. The elemental analysis as obtained from EDX is in close agreement with the starting composition used for the synthesis. The EDX quantification can be influenced by the surface crystalline defects of the nano-particles. This can also be taken into account to explain the difference between the values of the atomic ratio as determined by EDX and the expected value. The EDX pattern confirmed the homogeneous mixing of the Mg, Ni and O atoms in doped sample. The observed composition is almost equal to that of the sample produced by stoichiometric calculations.

References

01) D. C. Johnston, H. Prakash, W. H. Zachariasen and R. Viswanathan Matters. Res. Bull. 8 (1973) 777.

02) S. Kondo, D. C. Johnston, C. A. Swenson, F. Borsa, A. V. Mahajan, L. L. Miller, T. Gu, A. I. Goldman, M. B. Maple, D. A. Gajewski, E. J. Freeman, N. R. Dilley, R. P. Dickey, J. Merrin, K. Kojima, G. M. Luke, Y. J. Uemura, O. Chmaissem and J. D. Jorgensen: Phys. Rev. Lett., 78 (1997) 3729.

03) N. Fujiwara, H. Yasuoka and Y. Ueda: Phys. Rev. B 57 (1998) 3539.

04) C. Urano, M. Nohara, S. Kondo, F. Sakai, H. Takagi, T. Shiraki and T. Okubo: Phys. Rev. Lett. 85 (2000) 1052.

05) K. Matsuno, T. Katsufuji, S. Mori, Y. Moritomo, A. Machida, E. Nishibori, M. Takata, M. Sakata, N. Yamamoto and H. Takagi: J. Phys. Soc. Jpn. 70 (2001) 1456.
06) Y. Ueda, N. Fujiwara and H. Yasuoka: J. Phys. Soc. Jpn. 66 (1997) 778.
07) S. H. Lee, C. Broholm, T. H. Kim, W. Ratcliff and S. W. Cheong Phys. Rev. Lett. 84 (2000) 3718.
08) N. Stubicar, A. Tonejc and M. Stubicar, Journal of Alloys and Compounds, 370 (2004) 296-301.
09) M. Isobe and Y. Ueda, Journal of Alloys and Compounds 383 (2004) 85-88.
10) M. Isobe and Y. Ueda, Journal of the Physical Society of Japan, 71 (2002) 1848-1851.
11) H. Hoal, C. Kloc and E. Bucher, Journel of Solid State Chemistry 125 (1996) 216-223.

Research papers communicated so far from present investigations

- **Synthesis and Structural Analysis of Al-doped Qandilite (Mg_2TiO_4)**
  Alok Kumar Singh, *Ravi Kumar, T.D. Senguttuvan and Azher M. Siddiqui*
  AIP Conf. Proc. 1393, pp. 235-236.

- **Synthesis, Microstructural and Thermal analysis of inverse spinel compound Mg_2TiO_4, *Alok Kumar Singh,*** *T. D. Senguttuvan and Azher M. Siddiqui, Int. J. Adv. Res. Sci. Technol. Volume 2, Issue2, 2013, pp 95-97.*

- **Study of curious spiral like features in inverse spinel compound (Mg_2TiO_4)**
  Alok Kumar Singh, *T. D. Senguttuvan and Azher M. Siddiqui., Int. J. Adv. Res. Sci. Technol. Volume 2, Issue2, 2013, pp 63-66.*

- **Synthesis, Characterization and DC Conduction Mechanism in Inverse Spinel Compound (Mg_2TiO_4)**, **Alok Kumar Singh,** Anju Dhillon, T. D. Senguttuvan and Azher M. Siddiqui, *Int. J. of Curr. Engg. and Technol., Vol.4, No.1 PP. 399-404.*

- **Synthesis, Structural and Morphological Properties of New Spinel Compounds ($MgNi_2O_4$) Prepared via Citrate - Gel Auto Combustion Method, Alok Kumar Singh,** Anju Dhillon, T. D. Senguttuvan and Azher M. Siddiqui, *J. of Alloy & Compd. (Communicated).*

- **Synthesis, Electrical and Magnetic properties of Magnesium nickel oxide ($MgNi_2O_4$), Alok Kumar Singh,** Anju Dhillon, T. D. Senguttuvan and Azher M. Siddiqui, *J. of Alloy & Compd. (Communicated).*

Paper presented in Conference

- Attended the National seminar on "***Condensed Matter, Nuclear & High Energy Physics" February 18-19, 2011.*** Department of Physics, Jamia Millia Islamia, New Delhi, India.

- Attended the ***"International Conference On Advances In Condensed & Nano Materials, ICACNM- 2011" February 22, 23-26, 2011.*** Department of Physics, Panjab University, Chandigarh, India.

- Attended the National seminar on "***Condensed Matter, Nuclear & High Energy Physics"*** Department of Physics, Jamia Millia Islamia, New Delhi, India.

- Attended the ***"International Conference and workshop on Nano-structured Ceramics and Other Nano-materials, ICWNCN- 2012" March 13-16, 2012.*** Department of Physics & Astrophysics, University of Delhi, New Delhi, India.